New Two-dimensional Phase of Boron with Anisotropic Electric Conductivity

Zhi-Hao Cui[1,2], Elisa Jimenez-Izal[1,3] and Anastassia N. Alexandrova[1,4]*

[1] Department of Chemistry and Biochemistry, University of California, Los Angeles, 607 Charles
E. Young Drive, Los Angeles, California 90095-1569, United States
[2] College of Chemistry and Molecular Engineering, Peking University, 100871 Beijing, China
[3] Kimika Fakultatea, Euskal Herriko Unibertsitatea (UPV/EHU), and Donostia International Physics Center (DIPC), P. K. 1072, 20080 Donostia, Euskadi, Spain
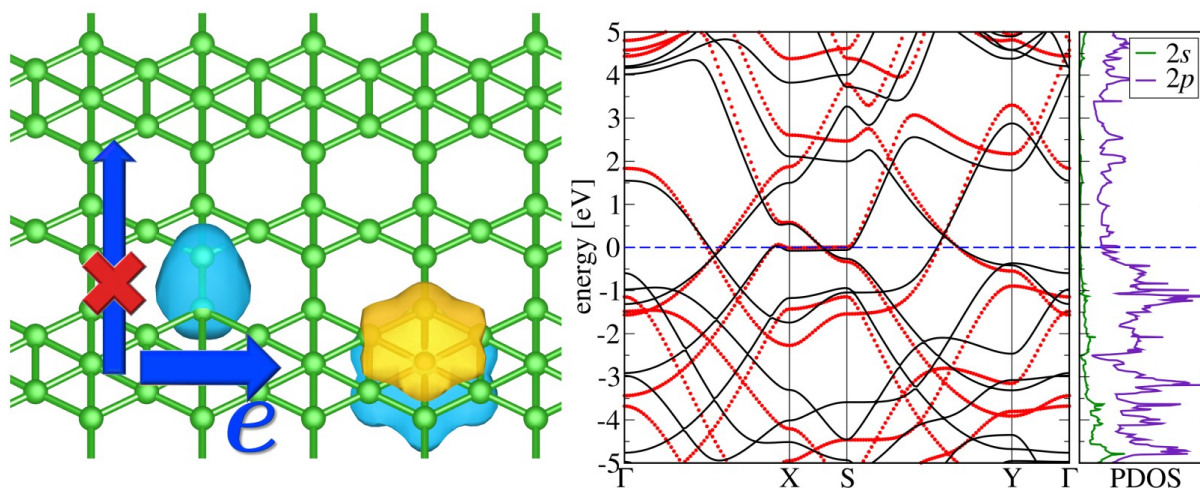[4] California NanoSystems Institute, Los Angeles, California 90095-1569, United States

Corresponding Author

[*]E-mail: ana@chem.ucla.edu

Two-dimensional (2D) phases of boron are rare and unique. Here we report a new 2D all-boron phase (named the π phase) that can be grown on a W(110) surface. The π phase, composed of four-membered rings, and six-membered rings filled with an additional B atom, is predicted to be the most stable on this support. It is characterized by an outstanding stability, and unusual electronic properties. The chemical bonding analysis reveals the metallic nature of this material, that can be attributed to the multi-centered π-bonds. Importantly, the calculated conductivity tensor is anisotropic, showing larger conductivity in the direction of the sheet that is in-line with the conjugated π-bonds, and diminished in the direction where the π-subsystems are connected by single σ-bonds. This work predicts a possibility of the substrate-assisted growth of a new 2D boron phase, whose unique electronic properties may be utilized in the electronic devices.

TOC GRAPHICS

KEYWORDS

Boron, 2D, anisotropic conductivity, DFT.

In the past decades, the outstanding geometry and electronic properties of graphene inspired a wide interest in low-dimensional structures[1,2]. However, for elements right next to carbon in the Periodic Table: silicon, boron, and phosphorus, the preparation of elemental 2D phases has been proven to be much more difficult[3–5]. Among these elements, boron is particularly intriguing and challenging. First, the elemental allotropes of boron are dominated by the well-known and very stable B_{12} icosahedral clusters[6]. Second, the 2D nature has been found to prevail only in small clusters of boron, governed by a mix of covalent and delocalized bonds in an undercoordinated situation[7,8]. Planarity does not easily translate to extended systems, because of the electron-deficient nature of boron, as compared to carbon: like a metal, the metalloid boron tends to go toward 3D bulk. In purely theoretical works, a large amount of effort went into finding stable 2D boron phases, e.g. the α sheet[9,10], β sheet[9,10] and χ sheet[11,12], by different approaches, including cluster expansion (CE)[13], particle-swarm optimization (PSO)[13,14], and based on existing structural characteristics[15]. These works mainly focus on the boron monolayer, constraining the global optimization to two dimensions, and not considering the possibility of growing the boron phase on a substrate to support it. The substrate, however, plays a crucial role in experimental preparation of 2D boron sheets, which is one of the major differences between the boron sheets and graphene in the experiment. Only very recently, a few types of boron sheets have been synthesized on Cu foils[16], and on a Ag(111) surface[5,17] by chemical vapor deposition (CVD). In these cases, the exoticism of boron structures again implied the complexity of the bonding features. The substrate obviously dictates the structural and electronic preferences in these materials, and also the feasibility of their preparation. Accordingly, the possibly rich 2D chemistry of boron might be accessible through templating on different supporting surfaces.
In this work we focus on the most stable surface of tungsten, W(110), as a substrate for 2D boron growth. This surface features good stability and an outstanding performance in growth of carbon nanotubes[18]. Most importantly, while Cu and Ag surfaces have an hexagonal symmetry, W(110) has a rectangular symmetry. Therefore, it might be a promising support to obtain novel boron monolayers. Indeed, we found a unique new 2D sheet of boron that can be formed on the W(110) substrate and, upon exfoliation, retains its structure and stability up to strikingly high temperatures. We show that this phase possesses special electronic structure and anisotropic electric conductivity.

To identify the most stable structure of 2D boron on W(110), we applied the particle-swarm global optimization method to explore several different chemical compositions, varying the number of B atoms from 12 to 18 per supercell, within an area of 6.34 Å × 8.97 Å. In order to estimate the relative stabilities of different compositions, we calculate the cohesive energy,

$$E_c = \frac{E_{tot} - E_{i} - nE_B}{n}, \quad (1)$$

where E_{tot} is the total energy of the system with the boron sheet on the substrate, E_{sub} is the energy of pure W substrate, E_B is the energy of a single boron atom and n the number of B atoms. Note

that the specific product obtained in the chemical vapor deposition depends not only on the cohesive energy Ec, but also the condition of preparation, which determines the chemical potential of boron. The predicted global minima structures for each composition, and their corresponding cohesive energies are shown in Figure 1.
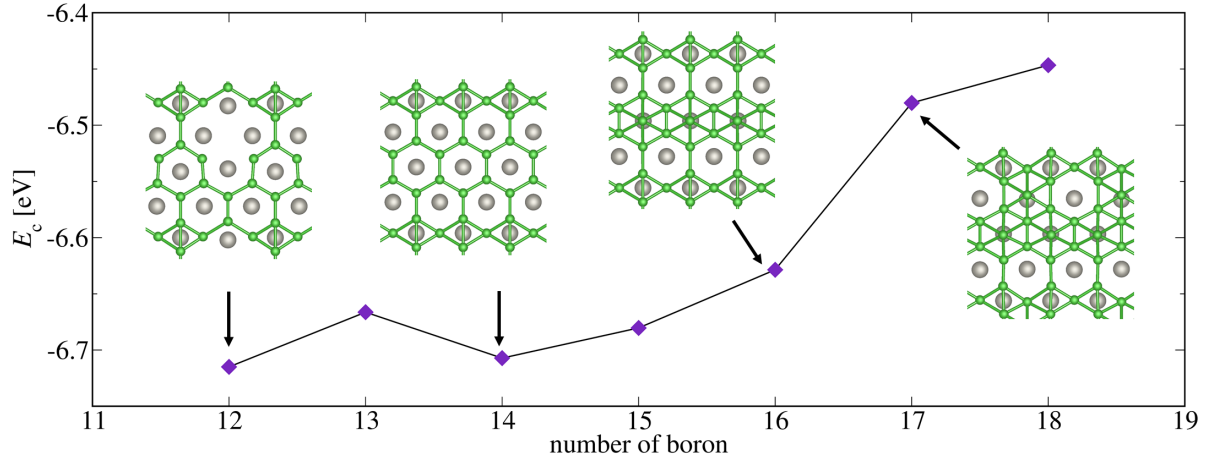

Figure 1. The cohesive energy is plotted as a function of the number of boron atoms. The representative structures are also labeled on the curve, where W and B atoms are depicted in gray and green respectively.

All the structures are based on a triangular lattice, where each boron is three or four-coordinated, a common feature in boron monolayers. Due to the symmetry of the W substrate, however, these structures are quite different from the ones reported previously[5,16,17]. Their most distinct feature is that they are composed of both four-membered and six-membered boron rings, where the formation of the four-membered rings can be regarded as a compromise in order to match the substrate structure as much as possible. First, boron atoms tend to form an epitaxial skeleton, matching the distribution of tungsten atoms. As the number of boron atoms increases, boron atoms fill the "holes" of the hexagons. Previous studies[9,15] found that filling all of the holes is unfavorable, due to the electron-deficient nature of boron. Our results further confirm this phenomenon by manually adding the boron atoms to the holes of the six-membered rings, which is found to be energetically unfavorable. Indeed, although the cohesive energy is still negative for the case where the number of boron atoms is larger than 16, its absolute value decreases significantly, indicating that the structure is unwilling to accept new boron atoms to fill the holes. Therefore, the structure containing 16 B atoms (Figure 2(a)), is thermodynamically more likely to be prepared in practice. To our knowledge, this structure has never been reported and we will hereafter refer to it as π sheet.
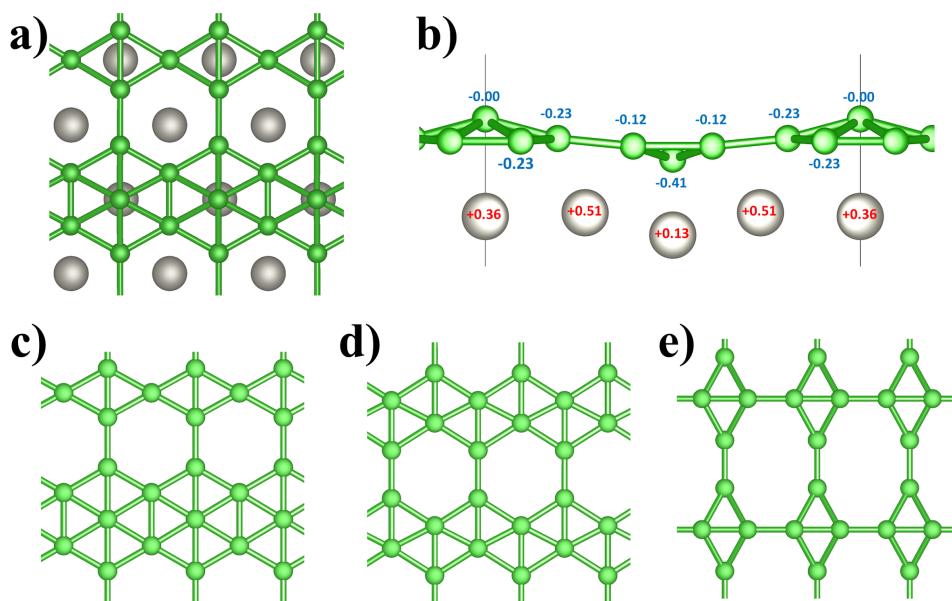
Figure 2. The π sheet and related structures: (a) top view and (b) side view (with Bader charges) of the π sheet on the substrate, (c) π sheet without the substrate, (d) χ_3 sheet and (e) the four-membered-ring structure.

Due to the interaction with the substrate, the π phase is slightly buckled (Figure 2 (b)); the Bader charge analysis shows a small charge transfer from the W surface to the boron sheet. Next, we analyze the π sheet without the substrate. Alone, this monolayer is a totally flat 2D material (Figure 2 (c)) and the phonon analysis, with no imaginary frequency mode (see Supplementary Information), confirms its dynamical stability. Additionally, ab initio MD simulations are performed at different temperatures in order to study the thermal stability of the new boron phase. These calculations suggest that the π sheet is stable up to 1800 K and only small buckling vibration, following the normal phonon mode, occurs with temperatures below 1800 K. Thus, the π sheet is a kinetically trapped, highly stable metastable polymorph. At 1800 K, the structure undergoes a phase transition and form the previously reported χ_3 structure[5,11,12] (see Figure 2 (d)), which is theoretically proven to be one of the most stable monolayers and has been prepared on a Ag(111) surface recently[5]. This phase is 0.05 eV/B atom more stable than the π phase without support. Nevertheless, on the W(110) substrate, the χ_3 sheet is less stable than the π sheet by ca. 0.13 eV/boron atom, due to the geometric mismatch between the χ_3 sheet and the W surface. This phenomenon shows again the great influence of the substrate on the 2D B and how the structural and electronic properties can be tailored by "playing" with the substrate.

It should be noted that with 16 boron atoms per supercell, a structure composed of only four-membered rings is also predicted (see Figure 2 (e)). Its stability is competitive with that of the π sheet while on the substrate. However, the four-membered-ring structure without the substrate is indeed unstable: (i) its energy is higher than the π sheet by ca. 0.31 eV/atom, and (ii) it shows a large imaginary frequency of 83 cm^{-1}, indicating dynamical instability.

Next we consider the electronic structure of the π sheet. First, we calculate the electronic band structure and the projected density of states (PDOS) (Figure 3). The band structure shows a metallic character, which is a common feature of 2D boron, despite the semiconductivity of the boron bulk. The results are similar when treating the band structure with PBE and hybrid functional HSE06, especially for the states near the Fermi level. This material is diamagnetic. From the PDOS analysis, the valence states are mainly 2p states hybridized with 2s states of boron. The main contribution to the states around the Fermi level arises from the $2p_z$ orbitals of B.
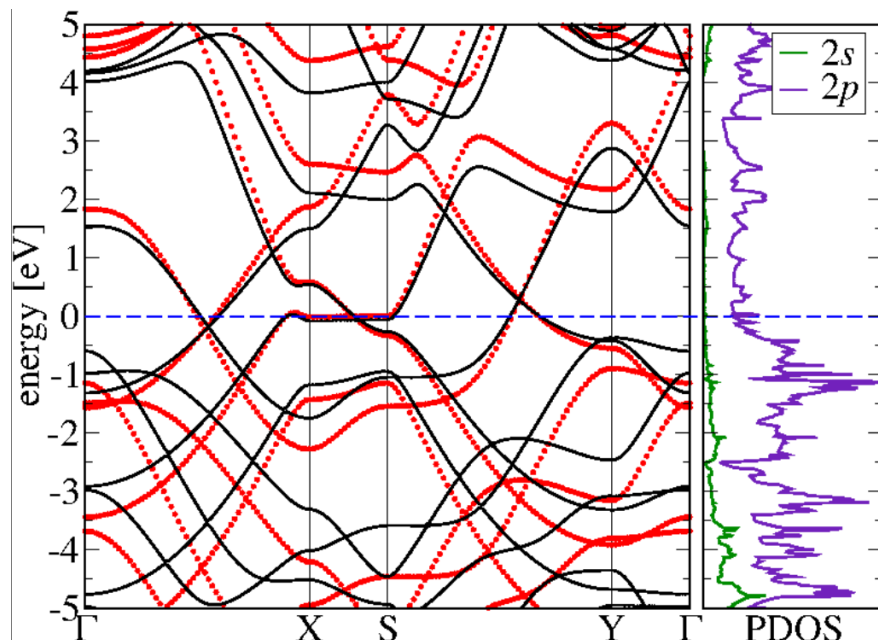

Figure 3. Electronic band structures and PDOS of the π boron sheet, where the black lines denote the result by PBE, the red dots denote the result by HSE06 and the blue dashed line indicates the Fermi level.

These features inspire us to establish a connection between the delocalized electronic band structure and the chemical bonds so that one can easily understand the electronic structures of 2D boron sheet from chemical intuition. The chemical bonding is analyzed using the SSAdNDP method, which maximally localizes the electron pairs into 1-, 2- and multi-centered bonds and the results are collected in Figure 4. The chemical bonding is quite similar to the elemental boron, with the formation of eight three-centered two-electron (3c-2e) σ bonds, with high occupation numbers (ON = 1.95-1.81 |e|) (Figure 4 (b), (c)). In general, B_3 can be viewed as the basic building block of the boron network. Additionally, one 2c-2e bond (ON = 1.79 |e|) plays a bridging role to connect the six-membered and the four-membered rings (Figure 4 (a)). The σ bonds are mainly composed of the sp^2 hybrid orbitals of boron, which agrees well with the 2s component peaks in the PDOS analysis. After forming the skeleton by these sp^2 hybrid orbitals, the remaining $2p_z$ orbital on each boron atom, have the potential to form delocalized π bonds. In

fact, we found two types of π bonds in the π sheet: one 4c-2e (ON = 1.74 |e|) and one 7c-2e bond (ON = 1.90 |e|), shown in Figure 4 (d) and (e). These delocalized π bonds provide a clear picture to understand the electronic structure of the boron sheet. First, the metallic character can be understood by the delocalized bonds. Second, the $2p_z$-dominated PDOS is obviously the result of these delocalized π bonds.
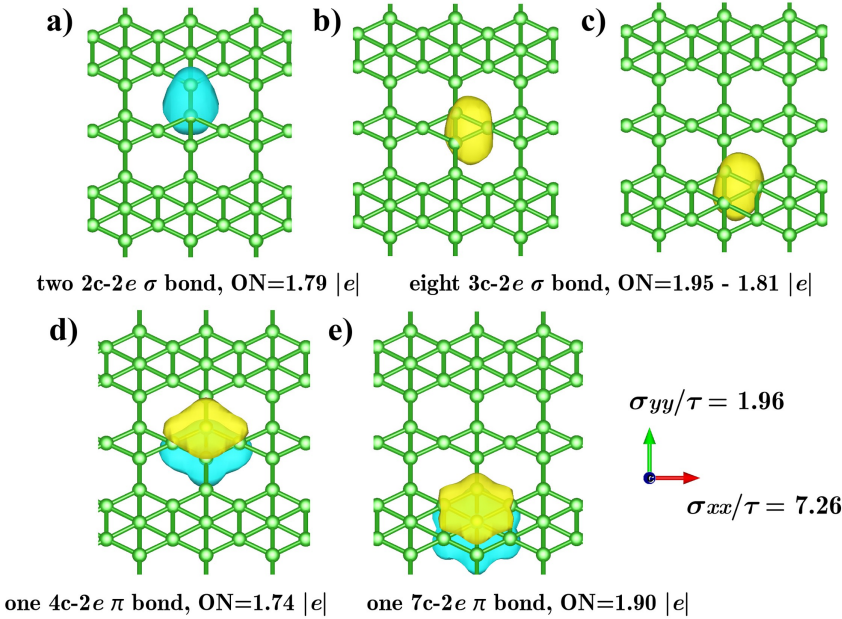

Figure 4. AdNDP chemical bonding analysis of the π boron sheet, where the "ON" denotes the occupation number. The number of different nc-2e of bonds in one primitive cell is also contained. In addition, the ratio of conductivity tensor component and the relaxation time (unit in $1019\ \Omega^{-1}m^{-1}\ s^{-1}$) is shown in the figure.

Further, as an evidence of this view, we calculate the conductivity tensor by solving the Boltzmann equation with relaxation time approximation[19]. It should be noted that there is still an unknown relaxation time τ in the denominator of conductivity, which is one limitation of the Boltzmann semi-classical approach. However, in this preliminary exploration of the transport properties, the relaxation time τ can be treated as a constant. Previous studies[20,21] have verified the validity of this approximation and implied that even for systems with highly anisotropic crystal axes, the approximation works quite well. According to the symmetry, the conductivity tensor is diagonalized. The components along the x and y axis at 300 K, listed in Figure 4, show that the conductivity along the x direction is approximately four times greater than that along the y direction. This can be easily understood from the bonding analysis: the x direction contains a continuous distribution of delocalized π bonds, while in the y direction, the π bonds are separated by 2c-2e σ bonds. As a result, the continuous delocalized bond distribution leads to a significantly larger conductivity in x direction, which makes the π sheet to be a potential anisotropic electric material. Notably the origin of the conduction in 2D boron sheet is quite similar to graphene, both caused by the delocalized π bonds. However, there are still two aspects

of difference: (i) the π boron sheet is anisotropic in conductivity, which may lead to interesting applications, and (ii) compared with graphene, the π bonds in boron sheets are intrinsically electron-deficient and the Fermi level can be easily modulated by doping with electron-rich atoms. We also calculate the case with slightly more electrons (higher chemical potential), and by doing so, the conductivity indeed increases to a large extent. Interestingly, when the chemical potential is ca. 0.22 eV above the Fermi level at 300 K, the conductivity along the x direction becomes twice as the non-doped case, however, the conductivity along the y direction is almost unchanged (Figure S3).

In summary, we propose a new structure, the π sheet, which is proven to be highly stable with or without the substrate, by phonon and MD simulations. In addition, the previously reported stable 2D structures of boron are not as stable as the π phase while on the W substrate. These findings show the importance of the substrate to template desired new 2D boron materials with tailored properties. The skeleton of this monolayer can be regarded as a result of multi-centered σ bonds. The metallic band structure and the 2p- dominated DOS arise from the formation of the delocalized π bonds by $2p_z$ orbitals of boron. The calculation of the transport properties further support this perspective by revealing the anisotropic conductivity, which might have important applications in electronic devices.

COMPUTATIONAL METHODS

The global optimization is performed by using the particle-swarm optimization (PSO) algorithm as implemented in the CALYPSO code[22,23]. PSO algorithm, initially inspired by the behavior of the bird flock, has been proven to be efficient in finding the global and local minima on sophisticated energy landscapes, not only for crystal structures[22,23], but also for the surface reconstructions[24]. In order to simulate the boron sheet on the tungsten substrate, the repeated slab model is used to describe both the surface region (including the boron sheet area constructed by the PSO algorithm and the buffer area in which the atoms are allowed to relax) and the bulk region (Figure S1). We used a rather large area of the W (110) surface (6.34 Å× 8.97 Å) to ensure the search space is large enough to include as many surface-boron structures as possible. The generated structures were optimized using the density functional theory (DFT) implemented in the Vienna ab-initio simulation package (VASP)[25]. PBE functional[26] was used for the structural relaxation and the stability check, including the phonon spectrum through the finite displacement approach[27] and the ab initio molecular dynamics (AIMD) simulations implemented in Quantum Espresso[28]. The DFT-D3[29] scheme was used to account for the dispersion interactions. The screened hybrid functional HSE06[30,31] was used for the electronic band structure calculation. The conductivity tensor was calculated using the Boltzmann semi-classical method by BoltzTraP code[19]. The chemical bonding analysis was performed by the Solid State Adaptive Natural Density Partitioning (SSAdNDP) method[32]. More details can be found in the Supplementary Information.

ASSOCIATED CONTENT

Supporting Information. Detailed information on the computational methods, phonon spectrum and phonon DOS of the π boron sheet and the conductivity tensor as a function of the chemical potential.

Notes

The authors declare no competing financial interests.

REFERENCES

(1) Geim, A. K.; Novoselov, K. S. The rise of graphene. *Nat. Mater.* **2007**, 6, 183–191.
(2) Castro Neto, A. H.; Guinea, F.; Peres, N. M. R.; Novoselov, K. S.; Geim, A. K. The electronic properties of graphene. *Rev. Mod. Phys.* **2009**, 81, 109–162.
(3) Zhao, J.; Liu, H.; Yu, Z.; Quhe, R.; Zhou, S.; Wang, Y.; Liu, C. C.; Zhong, H.; Han, N.; Lu, J.; Yao, Y.; Wu, K. Rise of silicene: A competitive 2D material. *Prog. Mater. Sci.* **2016**, 83, 24–151.
(4) Peng, X.; Wei, Q.; Copple, A. Strain-engineered direct-indirect band gap transition and its mechanism in two-dimensional phosphorene. *Phys. Rev. B* **2014**, 90, 085402–085412.
(5) Feng, B.; Zhang, J.; Zhong, Q.; Li, W.; Li, S.; Li, H.; Cheng, P.; Meng, S.; Chen, L.; Wu, K. Experimental realization of two-dimensional boron sheets. *Nat. Chem.* **2016**, 8, 563–568.
(6) Albert, B.; Hillebrecht, H. Boron: elementary challenge for experimenters and theoreticians. *Angew. Chem. Int. Ed.* **2009**, 48, 8640–8668.
(7) Zhai, H.-J.; Kiran, B.; Li, J.; Wang, L.-S. Hydrocarbon analogues of boron clusters planarity, aromaticity and antiaromaticity. *Nat. Mater.* **2003**, 2, 827–833.

(8) Carenco, S.; Portehault, D.; Boissière, C.; Mézailles, N.; Sanchez, C. Nanoscaled metal borides and phosphides: recent developments and perspectives. *Chem. Rev.* **2013**, 113, 7981–8065.

(9) Tang, H.; Ismail-Beigi, S. Novel precursors for boron nanotubes: the competition of two-center and three-center bonding in boron sheets. *Phys. Rev. Lett.* **2007**, 99, 115501–115504.

(10) Tang, H.; Ismail-Beigi, S. Self-doping in boron sheets from first principles: A route to structural design of metal boride nanostructures. *Phys. Rev. B* **2009**, 80, 134113–134121.

(11) Özdoğan, C.; Mukhopadhyay, S.; Hayami, W.; Güvenç, Z. B.; Pandey, R.; Boustani, I. The unusually stable B100 fullerene, structural transitions in boron nanostructures, and a comparative study of α- and γ-boron and sheets. *J. Phys. Chem. C* **2010**, 114, 4362–4375.

(12) Wu, X.; Dai, J.; Zhao, Y.; Zhuo, Z.; Yang, J.; Zeng, X. C. Two-dimensional boron monolayer sheets. *ACS Nano* **2012**, 6, 7443–7453.

(13) Zhang, Z.; Yang, Y.; Gao, G.; Yakobson, B. I. Two-dimensional boron monolayers mediated by metal substrates. *Angew. Chem.* **2015**, 127, 13214–13218.

(14) Yu, X.; Li, L.; Xu, X.-W.; Tang, C.-C. Prediction of two-dimensional boron sheets by particle swarm optimization algorithm. *J. Phys. Chem. C* 2012, 116, 20075–20079.

(15) Penev, E. S.; Bhowmick, S.; Sadrzadeh, A.; Yakobson, B. I. Polymorphism of two-dimensional boron. *Nano Lett.* **2012**, 12, 2441–2445.

(16) Tai, G.; Hu, T.; Zhou, Y.; Wang, X.; Kong, J.; Zeng, T.; You, Y.; Wang, Q. Synthesis of atomically thin boron films on copper foils. *Angew. Chem.* **2015**, 54, 15473–15477.

(17) Mannix, A. J.; Zhou, X. F.; Kiraly, B.; Wood, J. D.; Alducin, D.; Myers, B. D.; Liu, X.; Fisher, B. L.; Santiago, U,; Guest, J. R.; Yacaman, M. J.; Ponce, A.; Oganov, A. R.; Hersam, M. C.; Guisinger, N. P. Synthesis of borophenes: anisotropic, two-dimensional boron polymorphs. *Science* **2015**, 350, 1513–1516.

(18) Yang, F. Wang, X.; Zhang, D.; Yang, J.; Luo, D.; Xu, Z.; Wei, J.; Wang, J.-Q.; Xu, Z.; Peng, F.; Li, X.; Li, R.; Li, Y.; Li, M.; Bai, X.; Ding, F.; Li, Y. Chirality-specific growth of single-walled carbon nanotubes on solid alloy catalysts. *Nature* **2014**, 510, 522–524.

(19) Madsen, G. K. H.; Singh, D. J. BoltzTraP. A code for calculating band-structure dependent quantities. *Comput. Phys. Commun.* **2006**, 175, 67–71.

(20) Scheidemantel, T. J.; Ambrosch-Draxl, C.; Thonhauser, T.; Badding, J. V.; Sofo, J. O. Transport coefficients from first-principles calculations. *Phys. Rev. B* **2003**, 68, 125210–125216.

(21) Allen, P. B.; Pickett, W. E.; Krakauer, H. Anisotropic normal-state transport properties predicted and analyzed for high-tc oxide superconductors. *Phys. Rev. B* **1988**, 37, 7482–7490.

(22) Wang, Y.; Lv, J.; Zhu, L.; Ma, Y. Crystal structure prediction via particle-swarm optimization. *Phys. Rev. B* **2010**, 82, 094116–094124.

(23) Wang, Y.; Lv, J.; Zhu, L.; Ma, Y. CALYPSO: a method for crystal structure prediction. *Comput. Phys. Commun.* **2012**, 183, 2063–2070.

(24) Lu, S.; Wang, Y.; Liu, H.; Miao, M.-s.; Ma, Y. Self-assembled ultrathin nanotubes on diamond (100) surface. *Nat. Commun.* **2014**, 5, 3666–3671.

(25) Kresse, G.; Furthmüller, J. Efficient iterative schemes for ab initio total-energy calculations using a plane-wave basis set. *Phys. Rev. B* **1996**, 54, 11169–11186.

(26) Perdew, J. P.; Burke, K.; Ernzerhof, M. Generalized gradient approximation made simple. *Phys. Rev. Lett.* **1996**, 77, 3865–3868.

(27) Togo, A.; Tanaka, I. First principles phonon calculations in materials science. *Scripta. Mater.* **2015**, 108, 1–5.

(28) Giannozzi, P.; Baroni, S.; Bonini, N.; Calandra, M.; Car, R.; Cavazzoni, C.; Ceresoli, D.; Chiarotti, G. D.; Cococcioni, M.; Dabo, I. Dal Corso, A.; de Gironcoli, S.; Fabris, S.; Fratesi, S.; Gebauer, R.; Gerstmann, U.; Gougoussis, C.; Kokalj, A.; Lazzeri, M.; Martin-Samon, L.; Marzari, N.; Mauri, F.; Mazzarello R.; Paolini, S.; Pasquarello, A.; Paulatto, L.; Sbraccia, C.; Scandolo, S.; Sclauzero, G.; Seitsonen, A. P.; Smogunov, A.; Umari, P.; Wentzcovitch, R.M. QUANTUM ESPRESSO: a modular and open-source software project for quantum simulations of materials. *J. Phys.: Condens. Matter* **2009**, 21, 395502–395521.

(29) Grimme, S.; Antony, J.; Ehrlich, S.; Krieg, H. A consistent and accurate ab initio parametrization of density functional dispersion correction (DFT-D) for the 94 elements H-Pu. *J. Chem. Phys.* **2010**, 132, 154104–154119.

(30) Heyd, J.; Scuseria, G. E.; Ernzerhof, M. Hybrid functionals based on a screened coulomb potential. *J. Chem. Phys.* **2003**, 118, 8207–8215.

(31) Heyd, J.; Scuseria, G. E.; Ernzerhof, M. Erratum: "hybrid functionals based on a screened coulomb potential" [*J. Chem. Phys.* **2003**, 118, 8207]. *J. Chem. Phys.* **2006**, 124, 219906.

(32) Galeev, T. R.; Dunnington, B. D.; Schmidt, J. R.; Boldyrev, A. I. Solid state adaptive natural density partitioning: A tool for deciphering multi-center bonding in periodic systems. *Phys. Chem. Chem. Phys.* **2013**, 15, 5022–5029.